Feasibility of using nanotechnology to improve TIR satellite imagers

Final review

ESTEC 23rd November 2012

Study Overview

Objectives of activity

The objectives of this study are:

1. To assess the current state-of-the-art in space detector equipment miniaturisation (including nano-technologies e.g. QDIP, QWIP) for thermal infrared applications.
2. To assess the feasibility of using, and potential performance of quantum dot infrared photodetectors for space applications.
3. To identify potential technology developments in order to implement space-borne QDIPs.
4. Establish a roadmap for space application and qualification of QDIPs.

Task 1 – Literature review

- Review of TIR detector technologies employed or proposed for imaging & spectroscopy in space
  - Technology
  - Performance
  - Processes
  - Applications
  - ROM costs
  - Availability
  - Manufacturers/developers
  - Technology comparison

Task 2 – Requirements analysis

- Review & analysis of detection & focal plane requirements necessary for a space instrument measuring in the TIR
  - Current & future mission types
  - Spectral & spatial resolution
  - SNR
  - Radiometric performance
  - Spacecraft & instrument resources
  - Qualification & reliability

Mid-term review

- Passed, with revisions of D1 and D2 accepted
- T2SL identified as promising technology
- Agreement to include review of T2SL as well as QDIP technology in tasks 3 and 4 at zero cost to agency
- CCN issued for zero-cost extension (staff availability issues)

Task 3 – Performance assessment

- Investigation of QDIP state-of-the-art performance
- Feasibility of using QDIP technology for TIR space instruments against requirements derived in D2
- Performance comparison between QDIPs and other technologies
- TRL assessment
- Identification of research groups, organisations & industrial entities involved in QDIP development
- *All of the above was also implemented for T2SL technology and incorporated in D3*

Task 4 – Roadmap establishment

- QDIP roadmap from current status to implementation as a focal plane in a space instrument (TRL 8)
  - Application & potential gains – covered in D3
  - FPA requirements, architectures, resources
  - Technology development areas, critical elements, technology status & alternatives - D3 and D4
  - Space qualification issues – D3 and D4
  - Development strategy, schedule, investment requirements, risk assessment
  - Commercial evaluation
- *All of the above was also implemented for T2SL technology and incorporated in D4*

Final review

- Today!
- D5 – Final report in preparation – required to formally close review
- Executive summary to be issued post-review

Feasibility of using nanotechnology to improve TIR satellite imagers

Final review

ESTEC 23rd November 2012

Outline

- Introduction of Type II Superlattice (T2SL)
- Dark current and detectivity
- High operating temperature (HOT)
- Device configurations
- FPA review
- Space applications
- Conclusions

3 wishes for IR FPA

3 wishes?

HIGH TEMPERATURE OPERATION

SMALL PIXEL, HIGH UNIFORMITY LARGE ARRAY

LOW COST

Type II superlattice

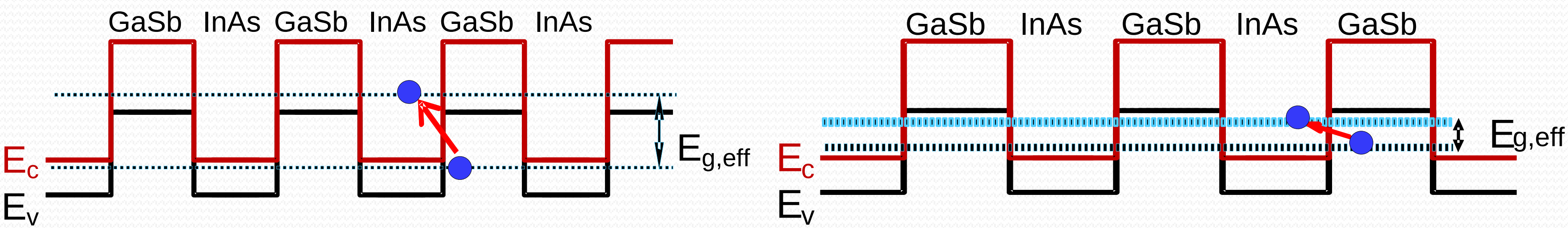

• High effective mass to reduce Auger recombination, leading to lower dark current and higher operating temperature

•Effective bandgap controlled by layer thicnesses, not alloy composition leading to high wafer uniformity

•Fabrication using III-V tools, so that small pixel for high format FPA can be achieved
•Availability of 4" (6" being developed) leads to lower cost.
•Growth of GaAs/Si could further lower the cost

Material	Si*	GaAs*	GaSb	InAs	InSb	CdTe	CdZnTe
Size	2" diameter					10mm×10mm	
Doping	undoped						Zn-doped
Orientation	(100)					(110)	
Price (US$)	39.95	59	450	475	495	399	459

Dark current comparison

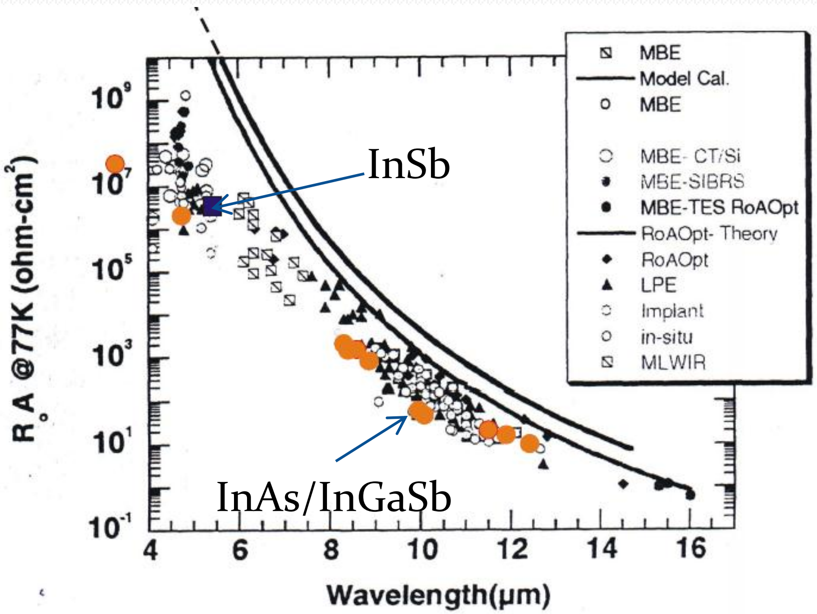

From [1]

•Dark current performance of T2SL approaches those from HgCdTe (MCT), Rule 07

• Dark current comparable to InSb in MWIR

•Dark current in T2SL mostly limited by surface leakage current although predominantly bulk current has been reported by some [2]

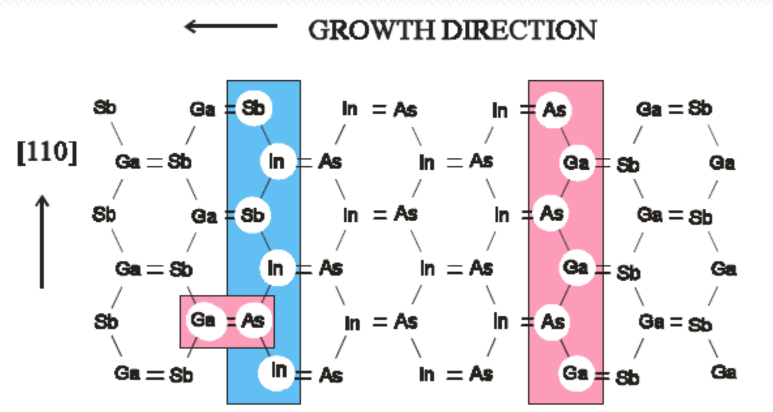

[1] P. Klipstein et al., "Antimonide-based materials for infrared detection," *Proc. SPIE*, vol. 4820, pp. 653–662, Jan. 2003.

[2] A. Hood et. al., "On the performance and surface passivation of type II InAs/GaSb superlattice photodiodes for the very-long-wavelength infrared," *Appl. Phys. Lett.*, vol. 87, p. 151113, Oct. 2005.

Detectivity

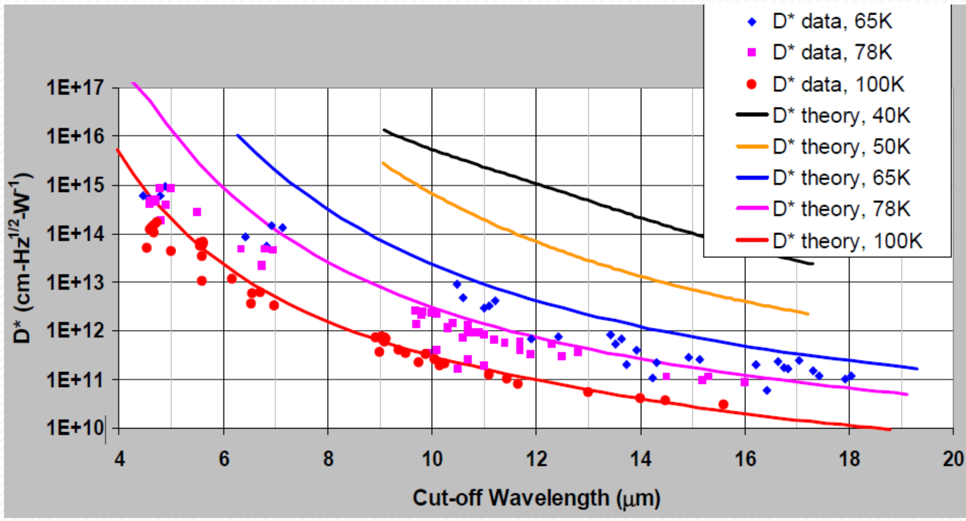

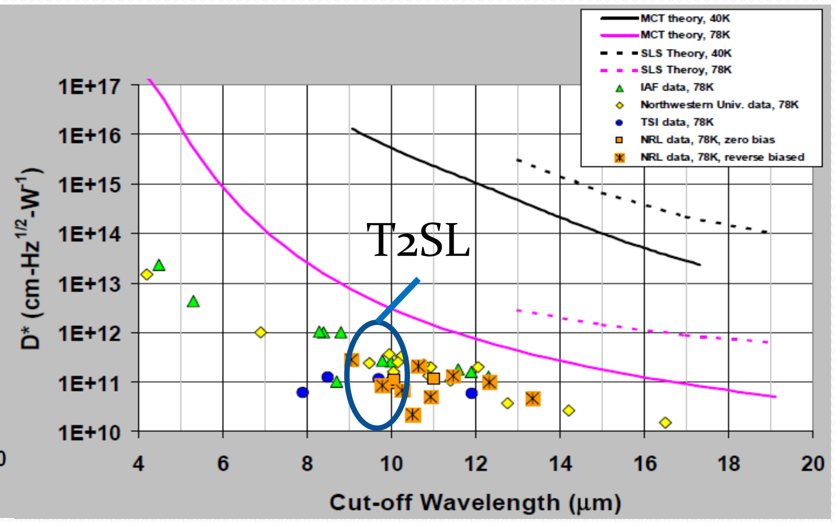

Measured and theory for thermally limited D* in MCT [3]

- At 77 K, D* approaches MCT at LWIR, but still lower at MWIR

- T2SL appears to be limited by high background doping (limited depletion width) and short carrier lifetime (>10 ns). InAs/InAsSb reported to have μs lifetime[4].

[3] J. Bajaj, G. Sullivan, D. Lee, E. Aifer, and M. Razeghi, "Comparison of type-II superlattice and HgCdTe infrared detector technologies," *Proc. SPIE*, vol. 6542, p. 65420B, May 2007.
[4] E. H. Steenbergen et al., "Significantly improved minority carrier lifetime observed in a long-wavelength infrared III-V type-II superlattice comprised of InAs/InAsSb," Appl. Phys. Lett., vol. 99, p. 251110, Dec. 2011.

High Operating Temperature (HOT)

Date, Affiliation, Reference	**Device Structure**	***T* (K)**	**λ_{cutoff} (μm)**	**QE**	**R_0A (Ω cm^2)**	**J_{dark} (A/cm^2)**	**D^* (Jones)**
Mar. 2005 Universite Montpellier II	- NIP - N^+: GaSb, 120nm - *i*: 10ML InAs/1ML InSb/10ML GaSb, 150x - P^+: GaSb, 120nm - T2SL intrinsic doping is *n*-type and 6e16 cm^{-3} at 300K	293	MWIR 5.9	R: 0.7mA/W @ 3.5μm	3e-2 @ 0V, 293K 0.5 @ 0V, 80K	N/A	N/A
Jul. 2012 University of New Mexico	- *i*-region: 7-stage cascade region with absorber, relaxation and interband tunneling regions per stage. - Absorber stage: 9ML InAs/9ML GaSb	77-**420**	MWIR 5.2 (77K, 100%), 7 (420K, 100%)	36.2% @ 4μm, 77K	N/A	3.6e-7 (77K), 7.3e-3 (295K) @ -5mV	5.3e10 (77K, 300K background, 2π FOV), 3e11 (77K, Johnson-noise limited), 8.9e8 (300K, Johnson-noise limited).
Jul. 1999 Northwestern University	- Photoconductive device - InAs/GaSb T2SL on **SI-GaAs**, LWIR.	**RT**	**12 (80%)**	6.02%	N/A	N/A	1.3e8 @ 11μm

High Operating Temperature (HOT)

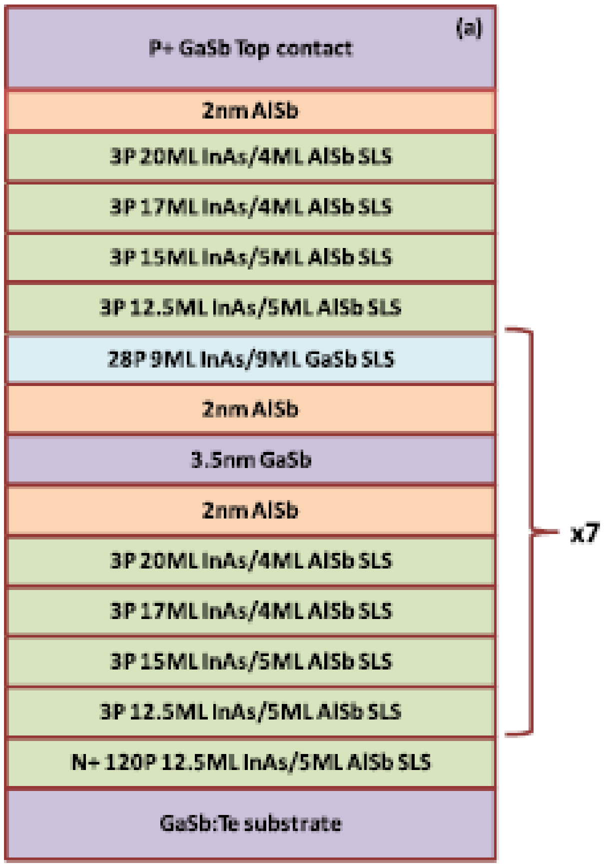

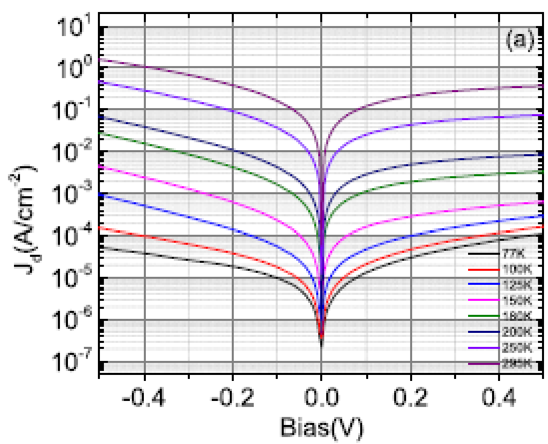

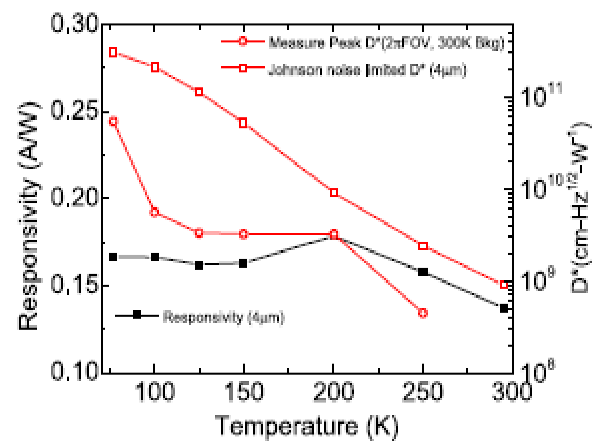

[5] N. Gautam et al., "High operating temperature interband cascade midwave infrared detector based on type-II InAs/GaSb strained layer superlattice," *Appl. Phys. Lett.*, vol. 101, no. 2, p. 021106, Jul. 2012.

More design options

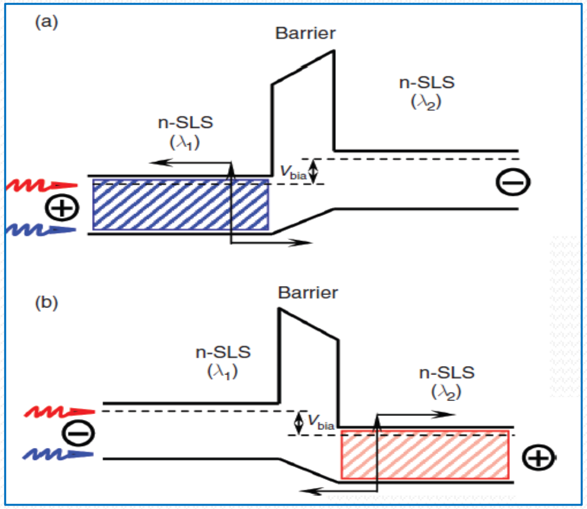

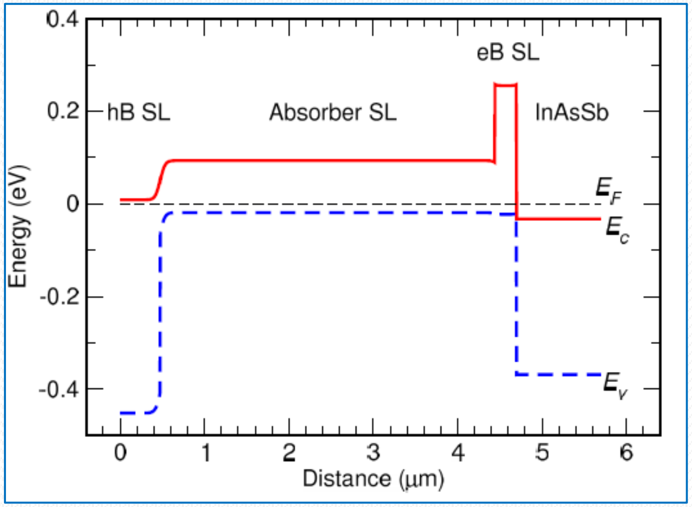

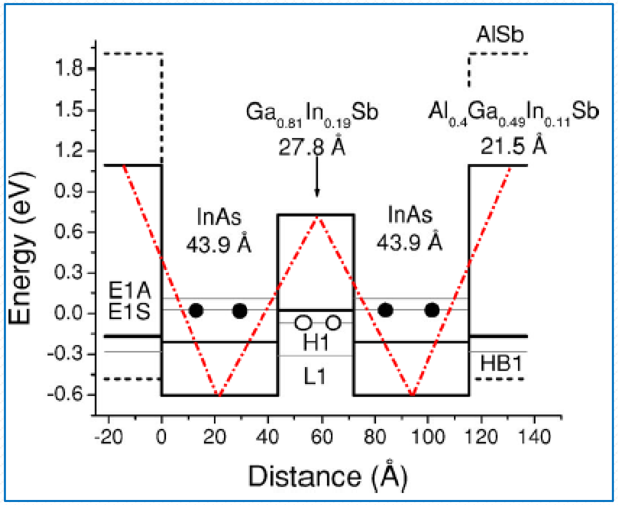

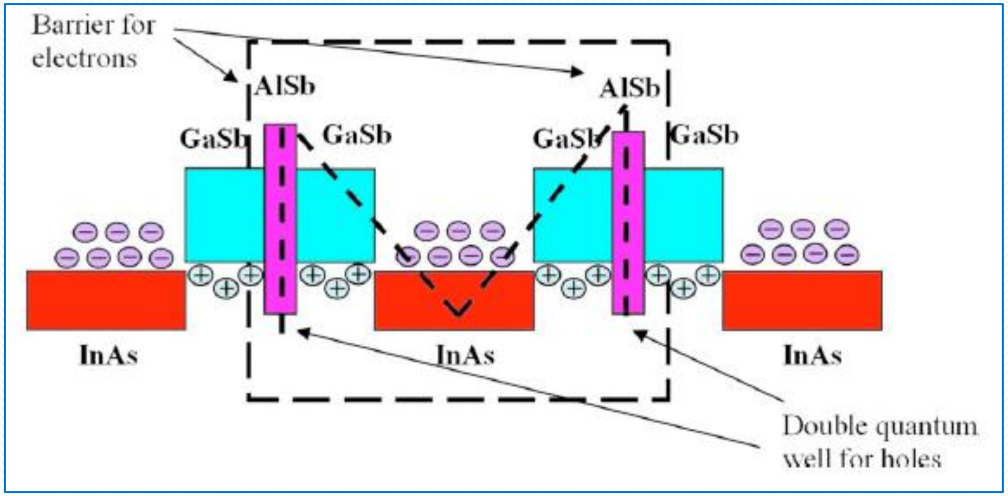

MWIR FPA

Date, Affiliation, Reference	Device Structure	*T* (K)	Bias (mV)	λ (µm)	QE	R_dA (Ω cm^2)	J_{dark} (A/cm^2)	D^* (Jones)	NETD (mK)	Array Dimensions and Operability
Jun. 2012 Northwestern University [74] Huang-OL	- InAs/GaSb T2SL - M-structure, PN heterojunction.	81	N/A	4.6 @ 77K (50%)	**70%**	N/A	N/A	N/A	**9-30**	- 320×256 pixels - Pixel size: 27µm **- Pixel operability: 99%** - Int. time: 2-13.5ms - Low-light conditions - photon flux 5e12 ph.cm^{-2}.s^{-1}.
May 2012 IRnova AB (Sweden) [75] Malm-SPIE	- InAs/Gab T2SL - homojunction PIN	110	-150	5.3 (~5%)	40% (max)	N/A	~1e-5 @ 0V ~1.6e-4 @ -150mV (G-R limited)	N/A	34	- 320×256 pixels - Pitch: 30µm **- Fill factor: 89.6%** - Int. time: 1.25ms
Aug. 2011 Fraunhofer IAF & AIM Infrarot-Module [76] Rehm-JEM	- InAs/GaSb T2SL on **3" GaSb** - NIPIN structure with a common ground *p*-type contact layer.	~77	N/A	4, blue channel 5, red channel	N/A	N/A		N/A	**17.9 (blue ch.) 9.9 (red ch.)**	- 288×384 pixels - Pitch: 40µm **- High wafer throughput and reproducibility** achieved by careful characterisation of full-wafer surface morphology and defects. - For missile warning systems application.
Apr. 2011 Northwestern University [77] Pour-APL	- InAs/GaSb T2SL - NIMP, M-structure.	150	**0**	4.2 (50%)	**50%**	5100 @ 0V	N/A	1.05e12	**11 @ ≤120K**	- 320×256 pixels - Int. time: 10.02ms - 300K background, f/2.3 optics, 2π FOV. **- BLIP @ ≤180K**

LWIR FPA

Date, Affiliation, Reference	Device Structure	*T* (K)	Bias (mV)	λ (μm)	QE	R_dA (Ω cm²)	J_{dark} (A/cm²)	D^* (Jones)	NETD (mK)	Array Dimensions and Operability
Jul. 2012 Jet Propulsion Laboratory [87] Rafol-JQE	- InAs/GaSb T2SL - *n*-type CBIRD structure.	78, 65	128	8.8 (50%)	**54% (max) @ 5.7 μm**	N/A	2.2e-4 @ 78K 1.1e-4 @ 65K	**1.3e11 @ 78K** **1.6e11 @ 65K**	**18.6 @ 78K** **12 @ 65K**	- 320×256 pixels - Pixel size: 27μm - Pitch: 30μm - Fill factor: 81% **- QE operability: 97%** - Int. time: 0.37ms - 298K background, f/2 optics
May 2012 QmagiQ (US) [8] Sundaram-SPIE	- InAs/GaSb T2SL	77	**-25**	~9.5	**50% (mean)**	N/A	~2e-4	N/A	30	**- 1024×1024 pixels** **- Pixel size: 16μm** **- Pitch: 18μm** - Pixel operability: 96% - f/4 optics
May 2012 Jet Propulsion Laboratory [88] Soibel-SPIE	- InAs/GaSb T2SL - *n*-type CBIRD structure.	77	**50**	10	**R: 2 A/W**	N/A	**<1e-5**	N/A	**26 @ 80K**	- 320×256 pixels **- Pixel operability: 98%** - 300K background
Jan. & Feb. 2012 Northwestern University [89] Haddadi-JQE [90] Haddadi-SPIE	- InAs/GaSb T2SL - M-structure	68, 81	**20 (81K)** **35 (68K)**	7.9	**81% (w/o AR coating, 81K)**	76 @ 81K 309 @ 68K	1.09e-3 (81K) 2.78e-4 (68K)	N/A	**27 @ 81K** **19 @ 68K**	**- 1024×1024 pixels** **- Pitch: 18μm** - Fill factor: 71.3% **- QE operability: 95.8% (81K), 97.4% (68K)** **- Weak low-*f* noise.** - Frame rate: 15Hz - Dynamic range: 37dB (81K), 39dB (68K) **- Int. time: 0.13ms** - 300K background, f/2 optics - ICP etched, SiO_2 passivated.

Present leading performance in T2SL

Detector Type	Window	R_0A or R_dA (Ω cm^2)	D^* (Jones)
Single-pixel devices	MWIR	>3×10^7 [43]	8×10^{13} [43]
	LWIR	~1×10^4 [10] – NIP 1.4×10^4 [63] – CBIRD	>1×10^{12} [6]
	VLWIR	0.55 [37] – NIP 837 [68] – InAs/GaInSbN T2SL	4.5×10^{10} [6]
FPA	MWIR	2.3×10^7 [83]	>1×10^{13} [85][86]
	LWIR	> 1×10^4 [64]	~1×10^{12} [91][92]

[6] F. Fuchs, U. Weimer, W. Pletschen, J. Schmitz, E. Ahlswede, M. Walther, J. Wagner, and P. Koidl, "High performance InAs/$Ga_{1-x}In_xSb$ superlattice infrared photodiodes," *Appl. Phys. Lett.*, vol. 71, no. 22, pp. 3251–3253, Dec. 1997.
[10] Y. Wei, A. Hood, H. Yao, V. Yazdanpanah, M. Razeghi, M. Z. Tidrow, and V. Nathan, "High-performance Type-II InAs/GaSb superlattice photodiodes with cutoff wavelength around 7 μm," *Appl. Phys. Lett.*, vol. 86, p. 091109, 2005
[43] C. J. Hill, J. V. Li, J. M. Mumolo, and S. D. Gunapala, "MBE grown type-II MWIR and LWIR superlattice photodiodes," *Infrared Phys. Technol.*, vol. 50, no. 2–3, pp. 187–190, Apr. 2007.
[63] D. Z.-Y. Ting, C. J. Hill, A. Soibel, S. A. Keo, J. M. Mumolo, J. Nguyen, and S. D. Gunapala, "A high-performance long wavelength superlattice complementary barrier infrared detector," *Appl. Phys. Lett.*, vol. 95, no. 2, p. 023508, Jul. 2009.
[64] D. R. Rhiger, R. E. Kvaas, S. F. Harris, B. P. Kolasa, C. J. Hill, and D. Z. Ting, "Characterization of barrier effects in superlattice LWIR detectors," *Proc. SPIE*, vol. 7660, p. 76601N, May 2010.
[68] L. Aina, H. Hier, A. Fathimulla, M. Lecates, J. Kolodzey, K. Goossen, M. Coppinger, and N. Bhargava, "High detectivity dilute nitride strained layer superlattice detectors for LWIR and VLWIR applications," *Infrared Phys. Technol.*, vol. 52, no. 6, pp. 310–316, Nov. 2009.
[83] R. Rehm, M. Walther, J. Schmitz, J. Fleissner, J. Ziegler, W. Cabanski, and R. Breiter, "Dual-colour thermal imaging with InAs/GaSb superlattices in mid-wavelength infrared spectral range," *Electron. Lett.*, vol. 42, no. 10, pp. 577 – 578, May 2006.
[85] M. Walther, R. Rehm, F. Fuchs, J. Schmitz, J. Fleißner, W. Cabanski, D. Eich, M. Finck, W. Rode, J. Wendler, R. Wollrab, and J. Ziegler, "256×256 focal plane array midwavelength infrared camera based on InAs/GaSb short-period superlattices," *J. Electron. Mater.*, vol. 34, no. 6, pp. 722–725, 2005.
[86] M. Walther, J. Schmitz, R. Rehm, S. Kopta, F. Fuchs, J. Fleißner, W. Cabanski, and J. Ziegler, "Growth of InAs/GaSb short-period superlattices for high-resolution mid-wavelength infrared focal plane array detectors," *J. Cryst. Growth*, vol. 278, no. 1–4, pp. 156–161, Apr. 2005.
[92] E. K. Huang and M. Razeghi, "World's first demonstration of type-II superlattice dual band 640x512 LWIR focal plane array," *Proc. SPIE*, vol. 8268, p. 82680Z, Jan. 2012.

Space applications: Scanning imaging multispectral

Instrument	Detector format	Bands (μm)	Array temp. (K)	NEP (W/Hz$^{1/2}$)	D* (cm.Hz$^{1/2}$W^{-1})
AATSR (Envisat)	Single pixel per TIR channel, 190 μm square	10.85, 12.0	80	~5x10^{-13}	3.8x10^{10}
ASTER (TERRA)	Ten pixels (offset linear) for each of the five TIR bands. 50 μm square pixels.	8.125-8.475 8.475-8.825 8.925-9.275 10.25-10.95 10.95-11.65	80	0.4x10^{-13} 0.4x10^{-13} 0.5x10^{-13} 1.1x10^{-13} 1.1x10^{-13}	1.3x10^{11} 1.3x10^{11} 1.0x10^{11} 4.5x10^{10} 4.5x10^{10}
JAMI (MTSAT-1R)	84 x 2 pixels – second column for redundancy. Pixels offset. 50 μm square pixels, 50 μm pixel column spacing.	3.5-4.0 6.5-7.0 10.3-11.3 11.5-12.5		6.9x10^{-13} 3.9x10^{-12} 6.9x10^{-12} 1.7x10^{-11}	7.3x10^{9} 1.3x10^{9} 7.3x10^{8} 2.9x10^{8}
SLSTR (Sentinel-3)	Two detectors per channel. Each pixel is 200 μm square.	3.74 (Δλ=0.38) 10.85 (Δλ=0.9) 12.0 (Δλ=1.0)	80	3.0x10^{-14} 6.3x10^{-13} 4.4x10^{-13}	6.7x10^{11} 3.7x10^{10} 4.6x10^{10}
MODIS (Terra, Aqua)	Each band has a ten-element linear array. Pixels are 540 μm square.	6.7 (Δλ=0.5) assumed 8.5 (Δλ=1) assumed 14.2 (Δλ=1) assumed	85	1.4x10^{-12} 2.4x10^{-12} 4.2x10^{-12}	3.9x10^{10} 2.3x10^{10} 1.3x10^{10}

T2SL is a feasible technology based on D*

Space applications: Pushbroom imaging multispectral

Instrument	Detector format	Bands (µm)	Array temp. (K)	NEP ($W/Hz^{1/2}$)	Comments	T2SL Feasibility
TIRS (LandSat-DCM)	Requirement is 1x1850 pixels. Implemented as three 640x512 pixel arrays. Each pixel is 25 µm square. Bands defined by filters directly above array.	10.8 12.0	43	6.7×10^{-13} 5.6×10^{-13}	Calculated. Assumptions made on throughput & optical efficiency. Bandpasses assumed to be 1 µm.	Yes
MSI (EarthCARE)	Requirement is 1x300 pixels per band. Implemented as a 384x288 pixel array. Each pixel on a 35 µm pitch.	8.8 (Δλ=0.9) 10.8 (Δλ=0.9) 12.0 (Δλ=0.9)		2.2×10^{-12} ←2.26×10^{-12} ←1.89×10^{-12} ←1.60×10^{-12}	←Calculated from quoted NETD ←Calculated required NEP. Assumptions made on throughput & optical efficiency.	Yes, if cooling is used.
IIR (CALIPSO)	320x240 pixel array. Only 64x64 pixels required. Each pixel is 51 µm square.	8.7 (Δλ=0.8) 10.5 (Δλ=0.8) 12.0 (Δλ=0.8)	Integrated cooler	8.5×10^{-12} 5.6×10^{-12} 4.6×10^{-12}	Calculated from quoted manufacturers NETD (f/1 optics, 30Hz frame). Actual image space f/# is 0.75.	Unknown as reported results are at ~80K for LWIR
NIRST (SAC-D/Aquarius)	Two linear arrays, each 512x3 pixels	3.8 10.85 11.85	Uncooled	4.6×10^{-12} 6.5×10^{-13} 5.4×10^{-13}	Calculated from quoted NETD and indications of bandwidth.	Appears not at present.

Space applications: Radiation

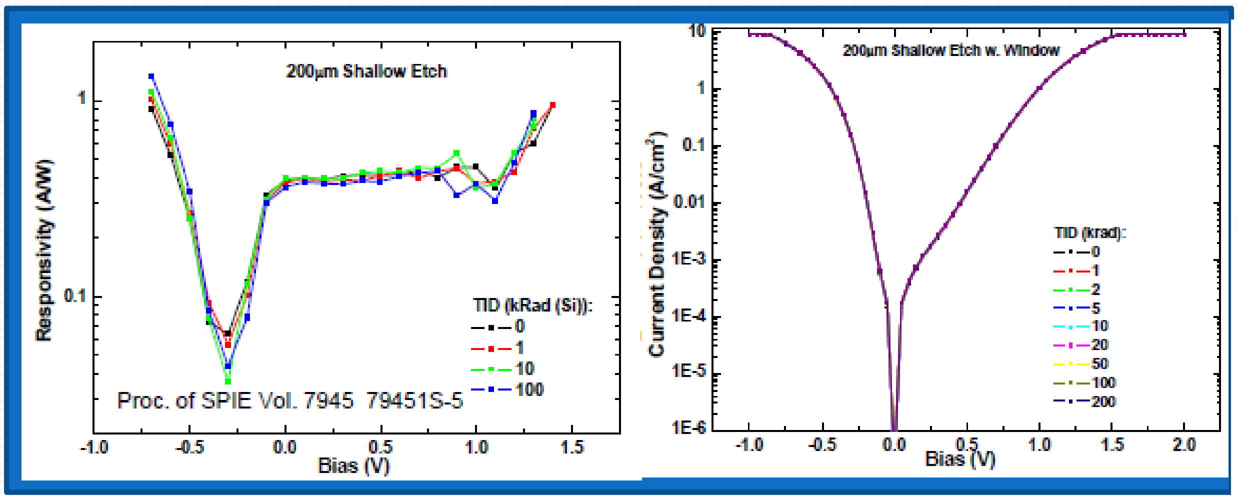

Gamma ray radiation

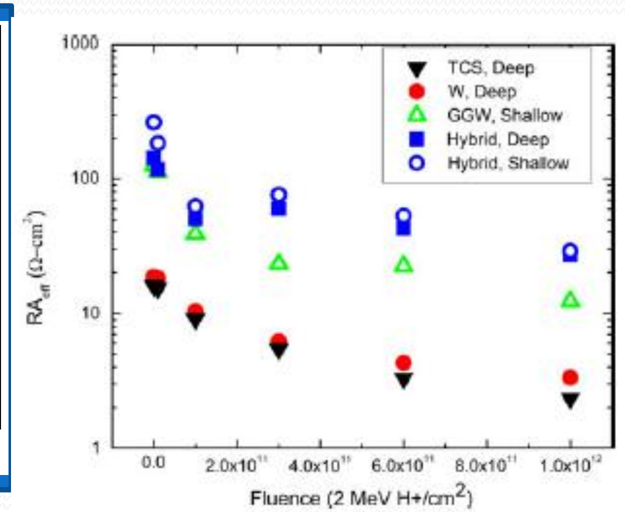

2MeV proton
TCS:Two constituent SL
GGW: graded bandgap in space charge region
Hybrid: TCS absorber + graded gap W

Conclusion

- Performance has improved rapidly over since 1990*.
- Dark current approaches HgCdTe Rule 07 and predicted to be lower.
- Detectivity at 77K competitive to HgCdTe, **NEDT 10-30mK, $t_{int} > 100\mu s$** .
- Uncooled detection at MWIR and LWIR demonstrated.
- Focal plane array up to Megapixel has been demonstrated.
- High design freedom based on a range of alloys.

Serious competitor to HgCdTe
Lower Cost ?(depends on substrates and manufacturers)
Good radiation hardness, potential in LWIR, VLWIR.

* R. H. Miles, D. H. Chow, J. N. Schulman, and T. C. McGill, "Infrared optical characterization of InAs/$Ga_{1-x}In_xSb$ superlattices," *Appl. Phys. Lett.*, vol. 57, no. 8, pp. 801–803, Aug. 1990

Feasibility of using nanotechnology to improve TIR satellite imagers

Final review

ESTEC 23rd November 2012

Outline

- Current QDIP performance
- Future QDIP performance
- Feasibility of using QDIP technology for TIR space instruments
- Space Qualification
- Conclusions

Current QDIP Performance

QDIP FPA Performance

Paper and Group	Structure details	Array dimensions and operability	Temp.(K)	Wavelength range	Bias	D* ($cmHz^{1/2}/W$)	NETD (mK)	QE	Id (A/cm^2)
Krishna et al., 2005. [1] **University of New Mexico, USA**	15 period InAs-InGaAs-GaAs DWELL structure GaAs substrate	320x256 pixels 30µm pitch >99% operability	78K	MWIR LWIR	+1.0V +2.6V	7.1×10^{10} 2.6×10^{10} (single pixel)	<100mK f/1 <100mK f/2		
Gunapala et al., 2007. [2] **Jet Propulsion Laboratory, USA**	30 period InAs-$In_{0.12}Ga_{0.88}As$- GaAs DWELL structure GaAs substrate	640x512 pixels 25µm pitch 23x23µm devices >99%operability	60K	LWIR 8.1µm peak	-0.35mV	~1×10^{10}	40mK f/2 optics t=20ms	5% mean	3×10^{-6}
Tsao et al., 2007. [3] **Northwestern University, USA**	25 period InAs-InGaAs-AlInAs DWELL structure InP substrate	320x256 pixels 30um pitch 25x25µm devices 99% operability	120-200K	MWIR Peak at 4µm	ROIC biases up to 3V	<1×10^{10} single pixel at 120K at >-2V	344mK at 120K f/2 optics t<30ms	1.1% conversion efficiency	
Vaillancourt et al., 2009. [4] **University of Massachusetts + QmagiQ, USA**	10 period InAs QD-$In_{0.2}Ga_{0.8}As$ barrier structure followed by 10 period InAs QD-GaAs barrier structure. GaAs substrate	320x256 pixels 30µm pitch 28x28um devices	67K	MWIR LWIR	-0.7V	1.8×10^{9} single pixel	172mK f/2.2 t=16.7ms		
Nagashima et al., 2009 [5] **Ministry of Defence, Japan + Fujitsu, Japan**	10 period InAs QD-$Al_{0.15}Ga_{0.85}As$ barrier structure GaAs substrate	256x256 pixels 40µm pitch >99.5% operability	80K	LWIR 10.3µm peak			87mK t=8ms, f/2.5 optics		
Andrews et al., 2011[6] **Naval Research Laboratory, USA + University of New Mexico + QmagiQ, USA**	30 period InAs-$In_{0.15}Ga_{0.85}As$-GaAs-$Al_{0.1}Ga_{0.9}As$ intermediate double DWELL structure, GaAs substrate	320x256 pixels 99.9% operability	60K	LWIR			106mK f/2 optics		
Lu et al., 2008 [7] **University of Massachusetts + Raytheon, USA**	10 period InAs QD-$In_{0.2}Ga_{0.8}As$ barrier structure followed by 10 period InAs QD-GaAs barrier structure. GaAs substrate	320x256 pixels 30µm pitch 27x27µm devices >90% operability		LWIR		2.3×10^{10} Single pixel			
Tang et al., 2006 [8] **Chung-Shan Institute of Science and Technology, Taiwan**	30 period InAs QD- GaAs barrier structure GaAs substrate	256x256 pixels >98% operability	80K	MWIR LWIR	0.3V	1.5×10^{10} Single pixel	Not given		~10^{-5} A/cm^2 Single pixel
Barve et al., 2011 [9] **University of New Mexico, USA**	30 period InAs-$In_{0.15}Ga_{0.85}As$-$Al_{0.08}Ga_{0.92}As$ DWELL structure GaAs substrate	320x256 pixels	80K	6.1µm peak		~4×10^{11} Single pixel	40mK f/2 optics		
Gunapala et al., 2011. [33] **Jet Propulsion Laboratory, USA**	Sub-ML InAs QD, GaAs QWs and AlGaAs barriers. GaAs substrate	1024x1024 pixels 19.5µm pitch	50K 60K 70K	8.5µm peak			22mK at 50K 28mK at 60K 33mK at 70K f/2 optics		

Dark Current comparison with QWIPs

- QDIPs compared to QWIPs detecting at similar wavelengths.
- QDIP dark current density lower than QWIPs for most of the electric field range

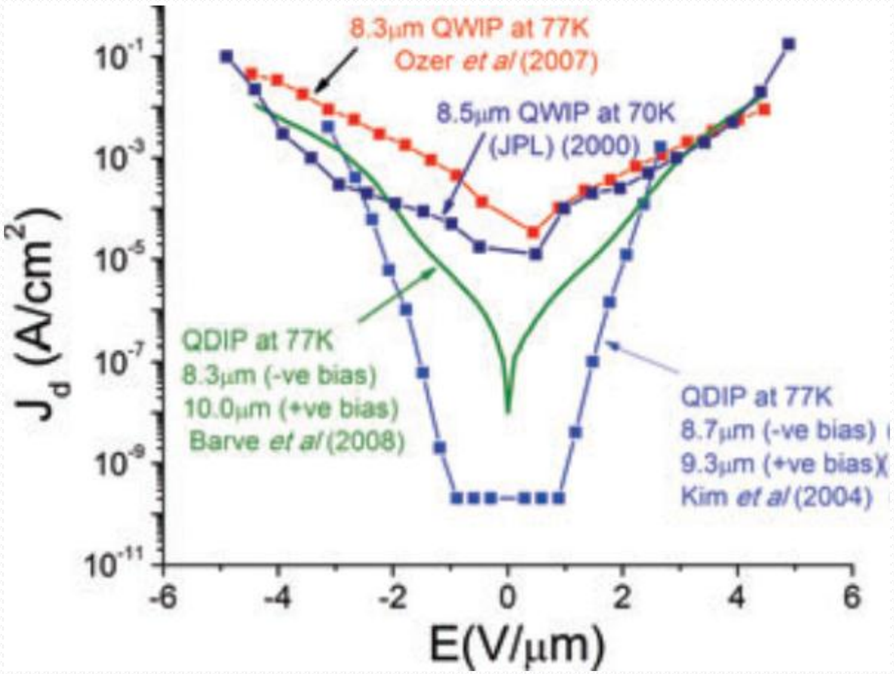

Future QDIP Performance

Future array dimensions

- 2048x2048 TIR FPAs reported as well as development of 4096x4096 HgCdTe FPAs.
- No fundamental problems to prevent similar sized QDIP FPAs.
- Mature III-V processing and low surface leakage should allow pixel sizes <20μm to be easily achieved.
- Operability already generally greater than 99%.

*D** improvement

- Reported 77-80K QDIP *D** values compared as function of wavelength
- Trend shows general *D** improvement over past 15 years.

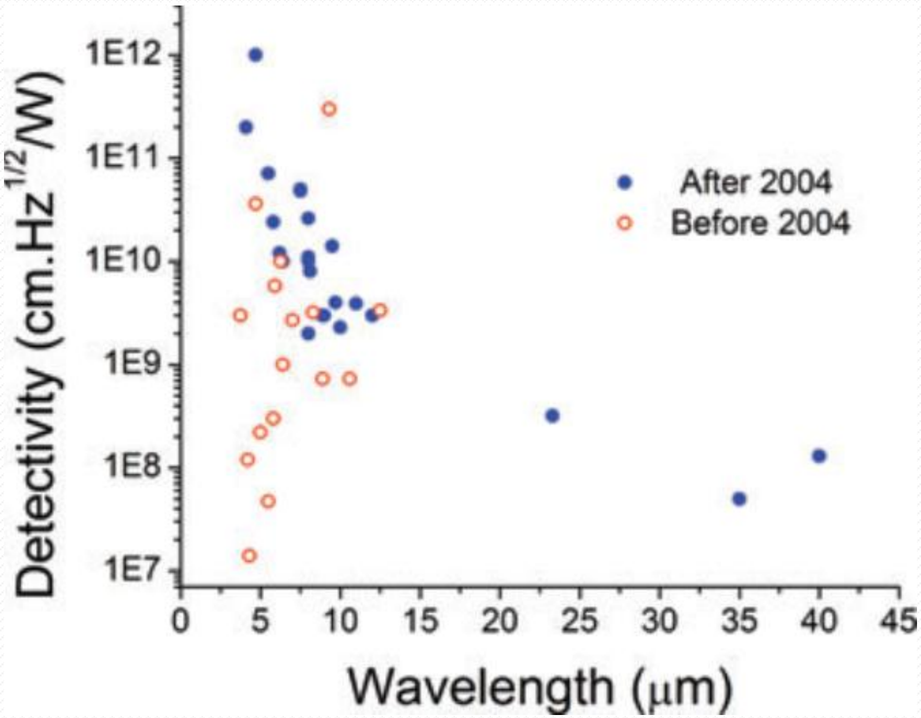

Metal Photonic Crystals

- Metal Photonic Crystals can be used to improve *D** and tune spectral response.
- Lee et al. [1] observed a 30 fold increase in D* compared to as grown QDIP.

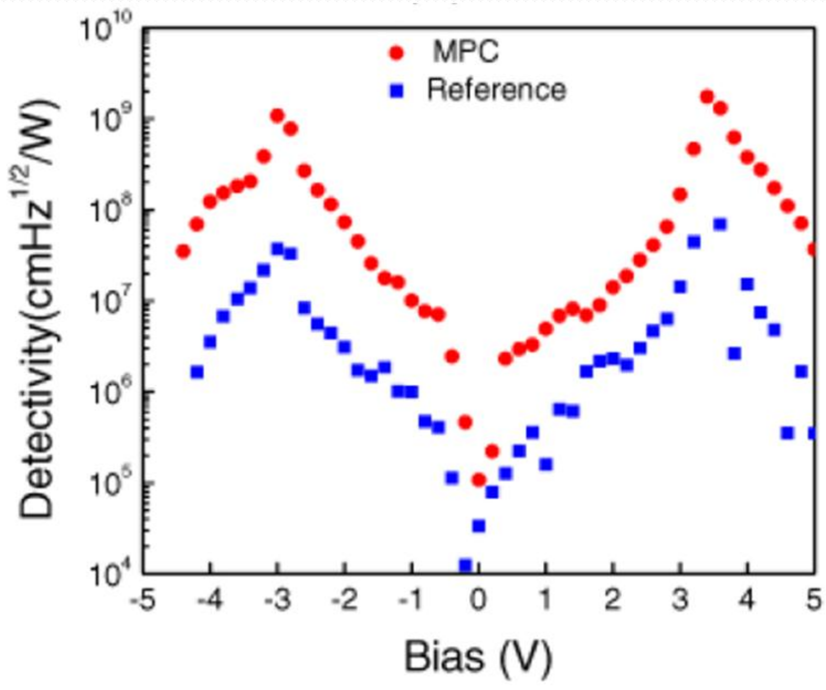

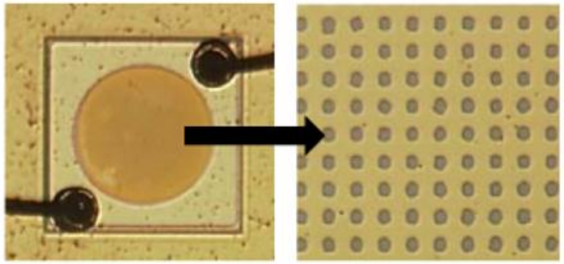

References:
[1] S. C. Lee *et al.*, *Optics Express*, vol. 17, p. 119407, 2009.

Theoretical *D**

- Models developed by Phillips [1], Martyniuk *et al.* and Ryzhii *et al.* [3], [4] to predict *D** in QDIPs as a function of wavelength and temperature.
- Assumptions:
  - QD are completely uniform in size and shape
  - Two energy states per QD
  - Carrier lifetime of 1ns

References:
[1] J. Phillips, *IEEE J. Quantum Electron.*, vol. 91, pp. 4590-4594, 2002.
[2] P. Martyniuk and A. Rogalski, *Prog. Quantum Electron.*, vol. 32, pp. 89-120, 2008.
[3] V. Ryzhii *et al.*, *Semicond. Sci. Technol.*, vol. 16, p. 331, 2001.
[4] V. Ryzhii *et al.*, *Appl. Phys. Lett.*, vol. 78, p. 3523, 2001.

Theoretical *D**

- QDIPs compared to HgCdTe and QWIPs at detection wavelengths of 5 and 10μm

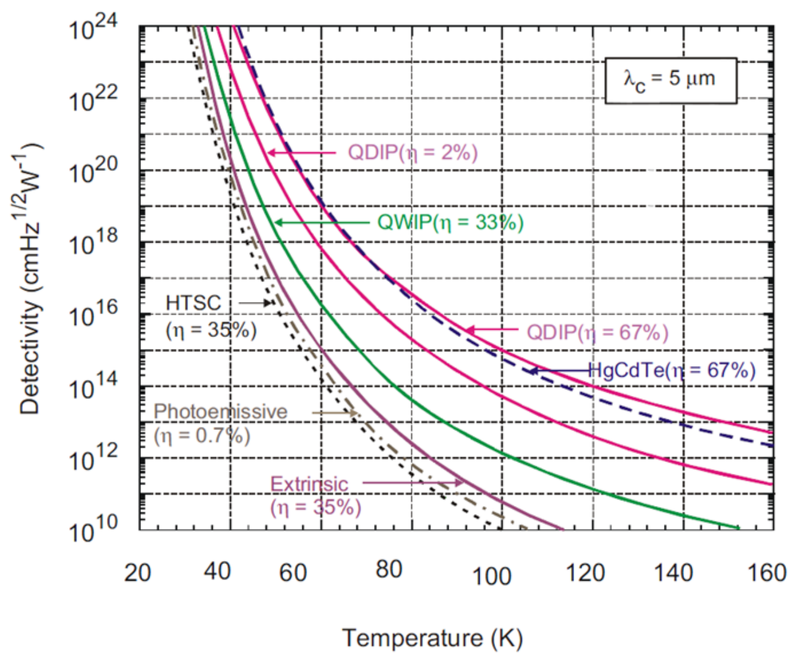

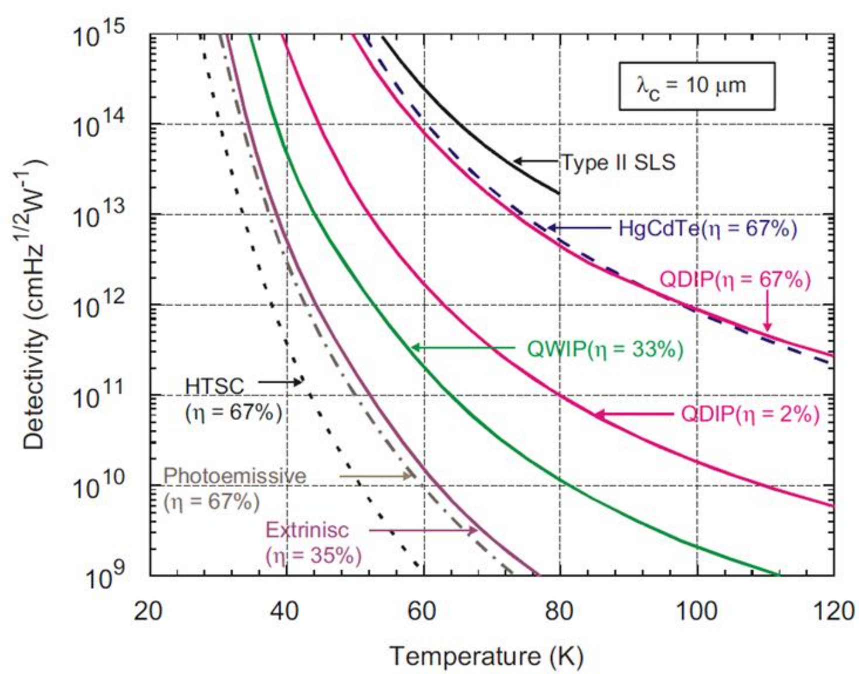

- Compares well to MCT if QDIP QE is assumed to 67%
- >1 order of magnitude higher than QWIPs if QDIP QE reduced to 2%

Theoretical *D** as function of T

- *D** as a function of T and cut off wavelength
- Again compares favourably with MCT

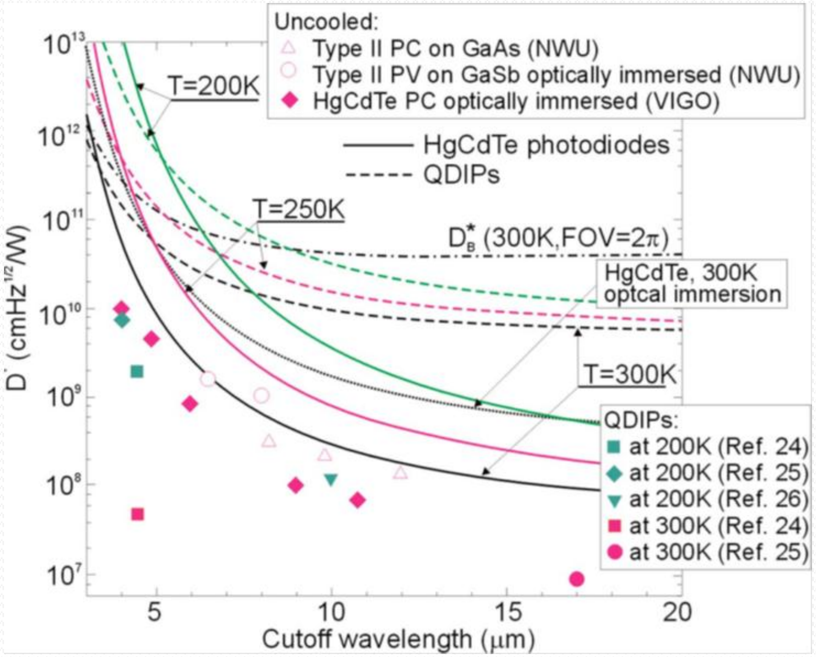

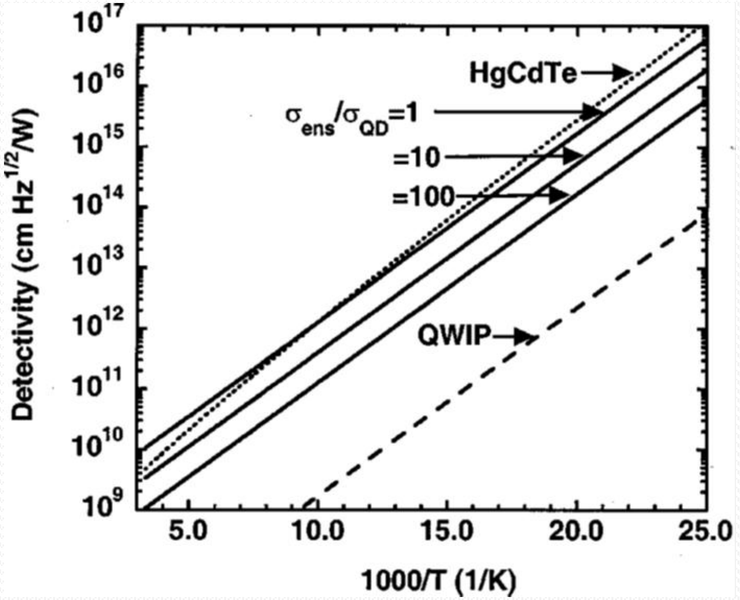

- Performance degrades rapidly if QD uniformity is decreased

Theoretical *D** and NETD

- Graph illustrates relationship between *D** and NETD
- Pixel non-uniformity has a large bearing on performance if NETD is low.

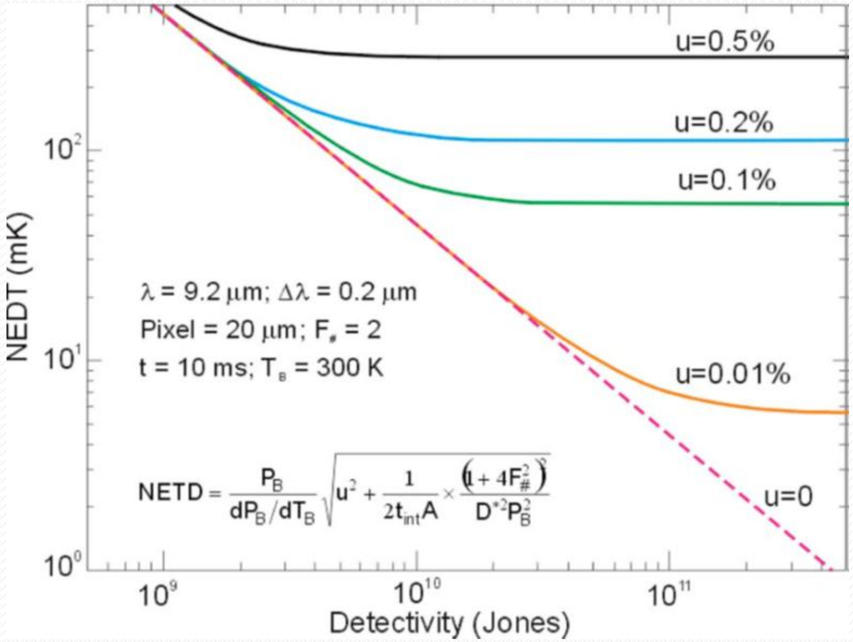

Dark Current Density

- Dark current density also predicted.

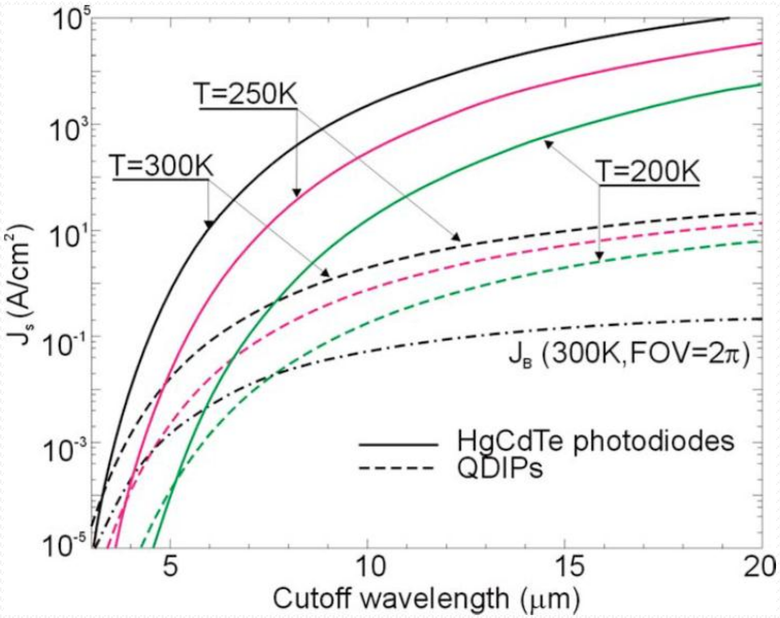

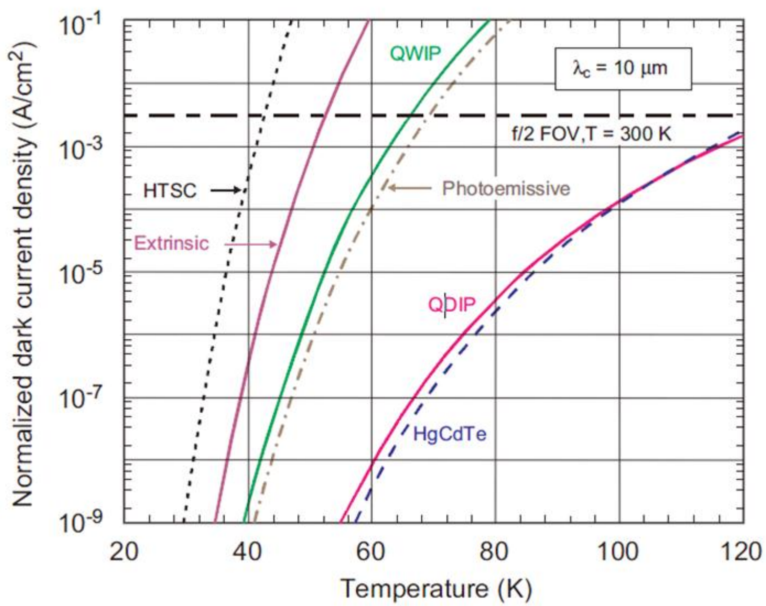

- Compares favourably with HgCdTe

QDIP improvements needed

- Several improvements are needed before QDIPs reach their predicted potential:
  - Improved QD uniformity
  - More control over QD doping
  - Greater absorption volume to achieve high QE
- These factors contribute to carrier lifetimes << 1ns assumed in model

Spectral Tuning

- QDIP's bias tunability can be exploited by a post processing algorithm for potentially high resolution spectroscopy.
- Complex spectral shapes have been reconstructed throughout the MWIR and LWIR ranges from QDIPs without need for optical filters.

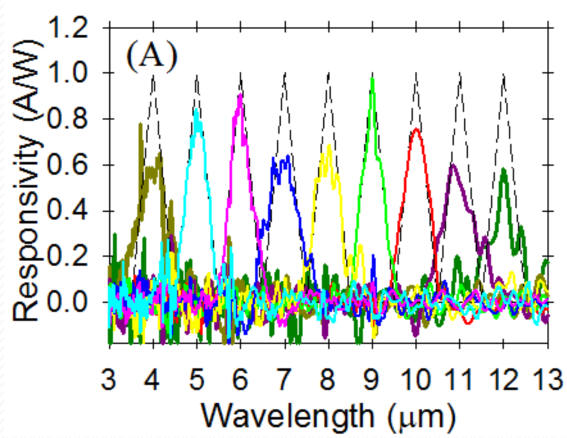

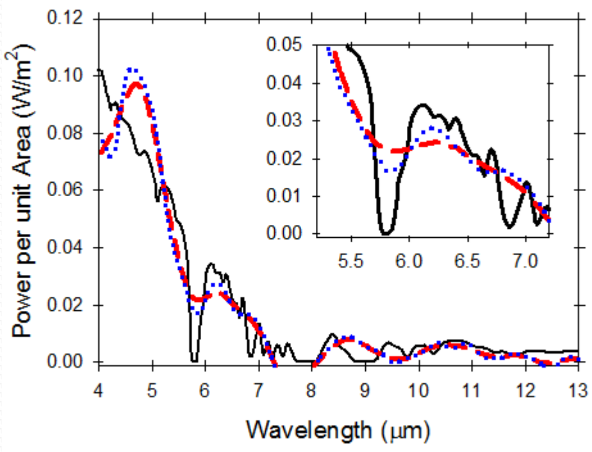

Feasibility of using QDIP technology for TIR space instruments

Scanning imaging multispectral radiometers

Instrument	Detector format	Bands (μm)	Array temp. (K)	NEP ($W/Hz^{1/2}$)	D^* ($cm.Hz^{1/2}W^{-1}$)
AATSR (Envisat)	Single pixel per TIR channel, 190 μm square	10.85, 12.0	80	~$5x10^{-13}$	$3.8x10^{10}$
ASTER (TERRA)	Ten pixels (offset linear) for each of the five TIR bands. 50 μm square pixels.	8.125-8.475 8.475-8.825 8.925-9.275 10.25-10.95 10.95-11.65	80	$0.4x10^{-13}$ $0.4x10^{-13}$ $0.5x10^{-13}$ $1.1x10^{-13}$ $1.1x10^{-13}$	$1.3x10^{11}$ $1.3x10^{11}$ $1.0x10^{11}$ $4.5x10^{10}$ $4.5x10^{10}$
JAMI (MTSAT-1R)	84 x 2 pixels – second column for redundancy. Pixels offset. 50 μm square pixels, 50 μm pixel column spacing.	3.5-4.0 6.5-7.0 10.3-11.3 11.5-12.5		$6.9x10^{-13}$ $3.9x10^{-12}$ $6.9x10^{-12}$ $1.7x10^{-11}$	$7.3x10^{9}$ $1.3x10^{9}$ $7.3x10^{8}$ $2.9x10^{8}$
SLSTR (Sentinel-3)	Two detectors per channel. Each pixel is 200 μm square.	3.74 ($\Delta\lambda$=0.38) 10.85 ($\Delta\lambda$=0.9) 12.0 ($\Delta\lambda$=1.0)	80	$3.0x10^{-14}$ $6.3x10^{-13}$ $4.4x10^{-13}$	$6.7x10^{11}$ $3.7x10^{10}$ $4.6x10^{10}$
MODIS (Terra, Aqua)	Each band has a ten-element linear array. Pixels are 540 μm square.	6.7 ($\Delta\lambda$=0.5) assumed 8.5 ($\Delta\lambda$=1) assumed 14.2 ($\Delta\lambda$=1) assumed	85	$1.4x10^{-12}$ $2.4x10^{-12}$ $4.2x10^{-12}$	$3.9x10^{10}$ $2.3x10^{10}$ $1.3x10^{10}$

Scanning imaging multispectral radiometers

- Potential of higher temperature operation. This has yet to be demonstrated in the LWIR band.
- Potentially more rugged, longer lifetime.
- Potential for greater uniformity.
- Potential for greater stability.

Pushbroom imaging multispectral radiometers

Instrument	Detector format	Bands (µm)	Array temp. (K)	NEP (W/Hz$^{1/2}$)	Comments
TIRS (LandSat-DCM)	Requirement is 1x1850 pixels. Implemented as three 640x512 pixel arrays. Each pixel is 25 µm square. Bands defined by filters directly above array.	10.8 12.0	43	6.7×10^{-13} 5.6×10^{-13}	Calculated. Assumptions made on throughput & optical efficiency. Bandpasses assumed to be 1 µm.
MSI (EarthCARE)	Requirement is 1x300 pixels per band. Implemented as a 384x288 pixel array. Each pixel on a 35 µm pitch.	 8.8 (Δλ=0.9) 10.8 (Δλ=0.9) 12.0 (Δλ=0.9)		2.2×10^{-12} ← 2.26×10^{-12} ← 1.89×10^{-12} ← 1.60×10^{-12}	←Calculated from quoted NETD ←Calculated required NEP. Assumptions made on throughput & optical efficiency.
IIR (CALIPSO)	320x240 pixel array. Only 64x64 pixels required. Each pixel is 51 µm square.	8.7 (Δλ=0.8) 10.5 (Δλ=0.8) 12.0 (Δλ=0.8)	Integrated cooler	8.5×10^{-12} 5.6×10^{-12} 4.6×10^{-12}	Calculated from quoted manufacturers NETD (f/1 optics, 30Hz frame). Actual image space f/# is 0.75.
NIRST (SAC-D/Aquarius)	Two linear arrays, each 512x3 pixels	3.8 10.85 11.85	Uncooled	4.6×10^{-12} 6.5×10^{-13} 5.4×10^{-13}	Calculated from quoted NETD and indications of bandwidth.

- QDIPs have sufficient sensitivity provided they can cover the necessary wavelength range.

Space Qualification

Space Qualification

- No specific studies on QDIPs.
- Predictions can be made due to similarities with QWIPs.
- QWIPs were used for the STRV-1d mission in 2000.
- QWIPs have been tested successfully for the Landsatt Data Community Mission.
- Since QWIPs can withstand the space environment it is probable that QDIPs can also.

Conclusions

- At present QDIPs show modest performance.
- Performance predicted to rival leading TIR detectors if growth challenges can be overcome.
- Number of small advantages for using QDIPs to replace HgTeCd devices in scanning imaging multispectral radiometers.
- Potential for QDIPs to be used in pushbroom imaging multispectral radiometers.
- It is probable that QDIPs will withstand space environment and launch.

Feasibility of using nanotechnology to improve TIR satellite imagers

Overview of Roadmapping : D4

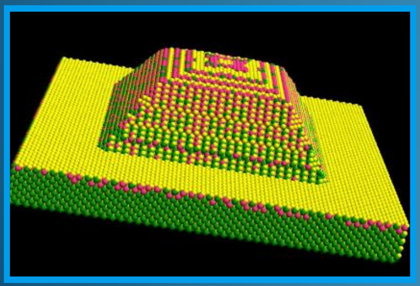

Quantum Dot Infra Red Photodetectors (QDIPs)

Research | **Development** | **Bespoke Production**

Material

MBE growth of Stranski-Krastanov dots with reduced density of non-radiative recombination sites. Incorporation and understanding of blocking barriers for dark current reduction. Polarisation and tunability investigation. Dual wave/Hyperspectral imaging . Dot size distribution.

Growth transition

Transfer to MOCVD process for large scale manufacture (transfer to commercial supply (e.g.IQE)).

For limited detector program (50 wafer level over three years) existing MBE capability could supply all material necessary

Space Qualification

Confirm increased radiation hardness advantage over QWIPs from previous QD/QW laser studies.

Initiate vibration studies

Modelling and Simulation

Extensive study has been made of the fundamental properties of dots, targeted at emitter technology (Lasers and LEDs). Whilst relevant, more IR detector specific modelling is required, particularly in strain and growth modelling to increase extent of active region. Modelling of bias dependence is essential for tunabiliyty to be exploited.

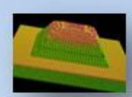

Single device processing

Dark current reduction via surface state passivation.

Device assessment for compatibility with existing QWIPs read out circuitry (key parameters R_0A and Q.E.).

Non planar device geometry (scatterer) similar to QWIPs. Contacting technology for device resistance reduction.

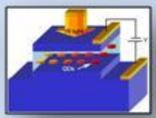

Camera

Housing, Drive electronics, software, all developed for QWIP and CMT detectors

Array processing

Hybridisation - Bump Bonding. Similar to QWIP devices.

Small 64x64 square array demonstrators at first.

Significant unknown issues are cross talk assessment

Move to larger 256x256 arrays and linear arrays for Pushbroom application

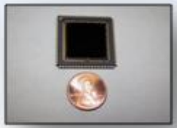

CMOS readout

Start with small 64 square array

QWIP compatible ROIC (pseudo off the shelf item).

Timeline

Type Two Superlattices (T2SL)

Research — Development — Bespoke Production

Material

Relating material defectsto dark current studeis
Studies of material defects related to pixel uniformity
New materials combination to reduce surface state leakage.
Growth onto highly mismatched substrates via IMF layers

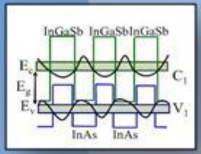

Growth transition

Translation to higher capacity growth capability is low risk (alr4eady been done from MBE to MOCVD in a number of other (emitter) areas.
Main study should focus on commercial viability commensurate with requirement and market need.

Space Qualification

Confirmation of radiation hardness
In particular focussing on the effect on surface leakage which for these devices could be critical

Modelling and Simulation

Use of complex band structure modelling inherited from cascade laser studies to engineer more precise quantum state alignment.

Single device processing

Low TRL study should critically be centred on the ralation of material properties (defects) with device dark current. Study should evolve around issues such as surface passivation, including field effect gating which shows promise.
Parameters limiting performance such as 1/f noise should be investigated.
Investigation of novel designs such as barrier blocking designs, and new W and M structures

Camera

Housing, Drive electronics, software, all developed for QWIP and CMT detectors

Array processing

Very few FPA issues have been addressed, but the similarity to QWIP handling means this is medium TRL. Hybridisation by bump bonding similar to QWIP devices.
Small 64x64 square array demonstrators at first moving rapidly to 256x256 arrays and larger.

CMOS readout

Start with small 64 square array
QWIP compatible ROIC (pseudo off the shelf item).

Timeline

EU Capability

- A number of 'capabilities' exist within the EU that can compete (technically) with the US.

- Selex Gallileo
  - Have developed infrared sensors for space applications (CMT)
  - Experience with producing QWIP sensors (GEC-Marconi Infra Red Laboratory – GMIRL)
  - *No III-V growth - would have to partner with growth facility (eg University of Sheffield in the UK)*
  - Little or no investment needed to produce array technology up to camera level.

EU Capability

- Thales/Sofradir
  - Established partnership (Sofradir supplying QW material to Thales)
  - Existing QWIP camera marketed (Catherine-MP thermal imager)
  - *Need to develop QDIP material or partner*
  - Little or no investment needed to produce array technology up to camera level.

- AIM/Fraunhofer (IAF)
  - Partnership that *already* produces type II cameras
  - Well positioned to produce FPA devices for space application

EU Capability

- IRnova (formerly part of Acreo) (Sweden)
  - Currently market QWIPs devices hybridised using FLIR readouts
  - Recent reports of type II devices (320x256)
  - *Currently Partner for Material supply*
  - Well positioned to provide III-V based FPA

- Xenics, (Belgium)
  - Currently Market cooled and uncooled thermal imaging cameras operating in the LWIR and MWIR wavebands.
  - Market QWIPs devices

EU Capability - Key Point

- Only viable if there are **performance** or **cost benefits**
- **Still a niche market, and so partnering and hanging on existing technology is crucial. Very little joined up capability without state/government support, or parallel funding.**

TRL - Status

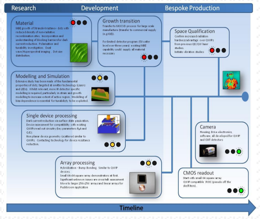

- **However usually for new technology**

Supply Chain

Material Devices Systems Products

TRL1-3/7-9 TRL4-6 TRL1-3/7-9

This is not true for either of these technologies

Quantum Dot Infra Red Photodetectors (QDIPs)

Research | **Development** | **Bespoke Production**

Material

MBE growth of Stranski-Krastanov dots with reduced density of non-radiative recombination sites. Incorporation and understanding of blocking barriers for dark current reduction. Polarisation and tunability investigation. Dual wave/Hyperspectral imaging. Dot size distribution.

Growth transition

Transfer to MOCVD process for large scale manufacture (transfer to commercial supply (e.g.IQE)).

For limited detector program (50 wafer level over three years) existing MBE capability could supply all material necessary

Space Qualification

Confirm increased radiation hardness advantage over QWIPs from previous QD/QW laser studies.

Initiate vibration studies

Modelling and Simulation

Extensive study has been made of the fundamental properties of dots, targeted at emitter technology (Lasers and LEDs). Whilst relevant, more IR detector specific modelling is required, particularly in strain and growth modelling to increase extent of active region. Modelling of bias dependence is essential for tunabiliyty to be exploited.

Single device processing

Dark current reduction via surface state passivation.

Device assessment for compatibility with existing QWIPs read out circuitry (key parameters R_0A and Q.E.).

Non planar device geometry (scatterer) similar to QWIPs. Contacting technology for device resistance reduction.

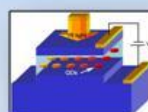

Camera

Housing, Drive electronics, software, all developed for QWIP and CMT detectors

Array processing

Hybridisation - Bump Bonding. Similar to QWIP devices.

Small 64x64 square array demonstrators at first.

Significant unknown issues are cross talk assessment

Move to larger 256x256 arrays and linear arrays for Pushbroom application

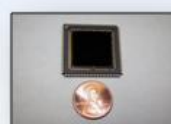

CMOS readout

Start with small 64 square array

QWIP compatible ROIC (pseudo off the shelf item).

Timeline

Type Two Superlattices (T2SL)

Research | **Development** | **Bespoke Production**

Material

Relating material defectsto dark current studeis
Studies of material defects related to pixel uniformity
New materials combination to reduce surface state leakage.
Growth onto highly mismatched substrates via IMF layers

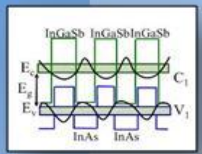

Growth transition

Translation to higher capacity growth capability is low risk (alr4eady been done from MBE to MOCVD in a number of other (emitter) areas.
Main study should focus on commercial viability commensurate with requirement and market need.

Space Qualification

Confirmation of radiation hardness
In particular focussing on the effect on surface leakage which for these devices could be critical

Modelling and Simulation

Use of complex band structure modelling inherited from cascade laser studies to engineer more precise quantum state alignment.

Single device processing

Low TRL study should critically be centred on the ralation of material properties (defects) with device dark current. Study should evolve around issues such as surface passivation, including field effect gating which shows promise.
Parameters limiting performance such as 1/f noise should be investigated.
Investigation of novel designs such as barrier blocking designs, and new W and M structures

Camera

Housing, Drive electronics, software, all developed for QWIP and CMT detectors

Array processing

Very few FPA issues have been addressed, but the similarity to QWIP handling means this is medium TRL. Hybridisation by bump bonding similar to QWIP devices.
Small 64x64 square array demonstrators at first moving rapidly to 256x256 arrays and larger.

CMOS readout

Start with small 64 square array
QWIP compatible ROIC (pseudo off the shelf item).

Timeline

Material

- Defect reduction research and understanding of non-radiative centres within the holding matrix, in particular time resolved luminescence measurements to study carrier relaxation mechanisms.
- Demonstration of saturated dot layers where the recapture length is less than the total device active layer thickness.
- Heterostructure engineering for resonant carrier escape mechanisms.
- Possible investigation into other growth modes that are better suited to uniformity

Growth Transition

- Assessment of requirement for commercial quantity.

Single Element Devices

- Novel geometries to enhance in plane absorption, similar to grating structures in QWIPs.
- Integration and investigation of Novel Plasmonic and Photonic Bandgap enhancement to absorption mechanisms (including the interaction of IR metamaterials with detector structures).
- Comprehensive examination of dark current mechanisms, origins and physical control.

Theoretical Study and Device Modelling

- Tailored modelling for strain compensation to increase dot absorption layers, specifically for IR absorption.
- Specific modelling for plasmonic or metamaterial enhancement to detection process

QDIPs

Focal Plane Arrays

- Cross talk studies of closely spaced (down to 15μm pitch) test arrays.
- Quantitative study of Pixel Uniformity for large arrays (→1024x768)

Space Qualification

- Confirming radiation hardness of these devices.
- Initiate vibration study – expected to be the same as QWIPs

Hybridisation

- No Significant Issues with current COTS technology
- Camera Electronics and Platform Housing

Camera Electronics and Platform Housing

- No Significant Issues with current COTS technology

QDIPs

Material

- The effect of dislocations on pixel operability and dark current
- Defect reduction research and understanding of non-radiative centres, in particular time resolved luminescence measurements to study minority carrier relaxation mechanisms.
- New strain relieving studies using IMF layers
- New material combinations to reduce surface conduction states

Growth Transition

- Assessment of requirement for commercial quantity.

T2SL

Single Element Devices

- Reliable device passivation to eliminate/minimise surface leakage currents (dark currents)
- Develop novel mesa structures to minimise dark current/ sidewall leakage
- Investigate and progress novel gated structures to minimise dark current/ sidewall leakage
- Systematic study of 1/f noise in T2SL diodes

Theoretical Study and Device Modelling

- Use band structure engineering developed for complex cascade laser designs to gain better predictive control of subband energies for complex T2 designs (such as W and M structures)

Focal Plane Arrays

- Growth onto large format GaAs material to enable III-V foundry processing to be utilised routinely

Space Qualification

- Confirming radiation hardness of these devices.
- Initiate vibration study – expected to be the same as QWIPs

Hybridisation

- No Significant Issues with current COTS technology

Camera Electronics and Platform Housing

- No Significant Issues with current COTS technology

T2SL

Conclusion

- EU capability exists that has experience in III-V IR FPA
- No complete joined up capability (like the US)

- T2SL seem to be more advanced than QDIPs (more people actually supply these as current offerings)

- Gains can be made by low TRL materials and single device research, stimulating commercial chain.

- Exploit advantages (**Tunability**)

Feasibility of using nanotechnology to improve TIR satellite imagers

Final review

ESTEC 23rd November 2012

D5 final report outline

What is required?

4.1.1. Final Report

The Final Report shall provide a complete description of all the work done during the study and shall be self-standing, not requiring to be read in conjunction with reports previously issued. It shall cover the whole scope of the study, i.e. a comprehensive introduction of the context, a description of the programme of work and report on the activities performed and the main results achieved.

4.1.4. Executive Summary Report

The Executive Summary Report shall concisely summarise the findings of the contract. It shall be suitable for non-experts in the field and should also be appropriate for publication. For this reason, it shall > not exceed five (5) pages of text and ten (10) pages in total (1500 to 3000 words).

We plan to provide:

- Final Report (D5) - Concise & informative summary of contract, as a standalone report
  - Summary of work carried out
  - Any deviations from SOW & reasons
  - Summaries & key conclusions of technical notes
    - Top-level descriptions of technologies, instrument types etc for a non-expert
    - Addressing all points in SOW
    - But in a clear and logical flow…easy reading!
  - Overall conclusions and recommendations
- And an executive summary – separate report - approx 5 pages.
- Format???